Spectral shape of stimulated Brillouin scattering in crystals

S. Ohno,[1,*] T. Sonehara,[1] E. Tatsu,[1] A. Koreeda,[2] and S. Saikan[1]

[1]*Department of Physics, Graduate School of Science, Tohoku University, Sendai 980-8578, Japan*

[2]*Department of Physical Sciences, College of Science and Engineering, Ritsumeikan University, Kusatsu 525-8577, Japan*

(Received 8 August 2015; published 11 December 2015)

We derived a formula to describe the stimulated Brillouin spectral shape in crystals for various temperatures ranging from room temperature to liquid-helium temperature. We modeled a sample as a one-dimensional system with a finite thickness in which the optically induced phonon propagates, partly interacting with the pump and probe laser beams. When the sample length is shorter than the propagation distance (i.e., the mean free path) of phonons, the spectral shape becomes multipeaked due to the multiple phonon reflections in the sample. Such a situation can be realized in a thin film or a bulk sample at low temperatures. We experimentally measured the Brillouin gain spectra with a multipeak structure in TeO_2 and $PbMoO_4$ crystals at low temperatures. We found that these spectra were reproduced by our formula for both the coaxial and off-axis phonon propagations with respect to the laser beams. It was revealed that our formula is very useful in estimating the phonon attenuation coefficient from the observed spectra, which gradually change from Lorentzian shape to a multipeak spectrum with decreasing temperature.

DOI: 10.1103/PhysRevB.92.214105 PACS number(s): 42.65.Es

I. INTRODUCTION

The progress of nanofabrication technology has shed fresh light on elementary excitations which arise in nanostructures, such as nanoparticles [1], nanowires [2,3], thin films [4,5], and superlattices [6,7]. These confined excitations provide us with new concepts in physics and they also have the potential for a wide range of applications in engineering. Phonon resonance, which is a main topic of this paper, is one of such confinement phenomena and it is characterized by both the propagation distance of the phonon and the finite size of the system, as will be mentioned later. Brillouin spectroscopy has been used as a powerful technique to nondestructively study the behavior of phonons in materials. The linewidth of a Brillouin spectrum is due to damping of the excitations, namely, the acoustic attenuation or phonon scattering in a medium.

We have developed a high-resolution Brillouin gain spectrometer with the spectral resolution of 20 kHz [8] and have improved it for high sensitivity by applying a frequency modulation (FM) technique [9]. Using this spectrometer, we demonstrated its high-resolution features and high sensitivity in measuring the temperature dependence of sound velocity in crystals [10], a two-level system in glasses [11], and some fundamental properties of crystals and amorphous materials [12–14]. In these studies, the principle of the stimulated scattering process, unlike the spontaneous one, enables precise measurements at low temperatures. In the stimulated process, the scattering signal does not decrease even at low temperatures with the reduction of thermal fluctuations. Koreeda and Saikan developed a spontaneous Brillouin spectroscopy balancing high spectral resolution with high-frequency shift measurement [15], but the stimulated scattering spectroscopy still has an advantage in the spectral resolution.

One issue that we found out, however, is the spectral shape of a bulk TeO_2 crystal, which appears as a several-peak spectrum at low temperature, as we reported previously [8]. In the early days of the research in Brillouin spectroscopy, Sandercock reported a similar spectral modulation of the spontaneous Brillouin spectrum in a thin film at room temperature [16]. He qualitatively discussed the reason for the appearance of the multipeak spectrum and proposed that it was due to the resonance of the sound wave within a thin film. In 1995, Sakai *et al.* investigated the thermal phonon resonance effect on the spontaneous Brillouin spectrum, in which many peaks appeared [17]. They applied the optical heterodyne technique to the spontaneous Brillouin scattering for the low-frequency phonon in liquid toluene. They proposed an insightful formula to explain the modulated spectra. In 2008, Minami *et al.* improved the formula for arbitrary reflectivity of the phonon at the ends of a resonant cavity and succeeded in reproducing the modulated spectra given in their experiments [18]. Recently, Rakich *et al.* reported gigantic enhancement of a stimulated Brillouin signal due to the phonons resonating with a nanoscale cavity [19].

In this paper, we first aim to elucidate an analytical formula to provide the Brillouin gain spectra of crystals at low temperature by revisiting the basics of the stimulated scattering process concerning the phonon confined in a finite volume. We then establish a methodology to obtain the essential Brillouin linewidth with respect to phonon scattering in the wide temperature range. Our final goal is to gain a unified and seamless understanding of spectral shape from normal damping to the resonance of the phonon in a stimulated Brillouin scattering process.

In general, the multipeak spectrum can be considered as a result of a resonance of elementary excitation in a finite system where the finesse varies continuously. In recent research, Brillouin spectroscopy has been applied not only for the acoustic properties, but also for magnetic properties via light scattering by the spin wave [20]. We believe that our proposed method is applicable to understand the resonance phenomena of these other elementary excitations as well.

*seigo@m.tohoku.ac.jp

In the next section, we derive a theoretical expression of the Brillouin gain spectrum under the premise that the counterpropagating light beams and the induced sound wave with coupling to each other are confined in a one-dimensional (1D) system. Then, we discuss how the spectral shape depends on the propagation distance of the sound wave, i.e., the mean free path of phonons, and it is shown that the different configurations of spatial overlap between the laser beams and the sound wave yield various spectral shapes. In the third section, we examine the validity of the derived expressions through the comparisons with the experimental results. Lastly, we present a summary and a conclusion of our study.

II. THEORY

A. One-dimensional system

In this section, we start from the wave equation of sound in a 1D medium. The sound wave is generated by counterpropagating laser beams: one is a probe beam whose angular frequency is ω_1 and the other is a pump beam of ω_2. The propagation direction is along the z axis, as shown in Fig. 1. This configuration models our experimental setup of a Brillouin gain spectrometer [8]. We can treat such a model with the wave equation for displacement $U_\Omega(z,t)$ with an external force as follows:

$$\frac{\partial^2 U_\Omega(z,t)}{\partial t^2} + \Gamma \frac{\partial U_\Omega(z,t)}{\partial t} - v^2 \frac{\partial^2 U_\Omega(z,t)}{\partial z^2} = C(z) e^{iqz - i\Omega t}, \tag{1}$$

where v, Ω, and Γ are the sound velocity in a medium, the sound frequency ($\Omega = \omega_1 - \omega_2$), and the phenomenological damping parameter, respectively. The right-hand side (rhs) of Eq. (1) describes the external force driven by the incident lasers. $C(z)$ represents the spatial distribution of the driving force or the interaction region.

We introduce a Green's function $G(z,t,z',t')$ such that the acoustic response of the 1D medium can be treated as follows:

$$\frac{\partial^2 G(z,t,z',t')}{\partial t^2} + \Gamma \frac{\partial G(z,t,z',t')}{\partial t} - v^2 \frac{\partial^2 G(z,t,z',t')}{\partial z^2} = \delta(z - z')\delta(t - t'). \tag{2}$$

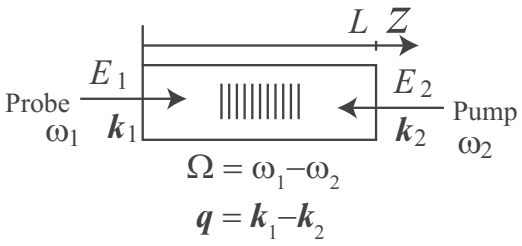

FIG. 1. Brillouin gain in a one-dimensional medium of length L. The electric field, angular frequency, and wave vector of the incident probe and pump beams are denoted by E_i, ω_i, and $\boldsymbol{k}_i$ ($i = 1, 2$), respectively. The external force oscillating with $\Omega = \omega_1 - \omega_2$, $\boldsymbol{q} = \boldsymbol{k}_1 - \boldsymbol{k}_2$ drives the sound wave.

Hence, a solution of $U_\Omega(z,t)$ can be formally written as follows:

$$U_\Omega(z,t) = \int_{-\infty}^{\infty} dt' \int_0^L dz' G(z,t,z',t') C(z') e^{iqz'} e^{-i\Omega t'} = \int_{-\infty}^{\infty} dt' G'(z,t,t') e^{-i\Omega t'},$$

where

$$G'(z,t,t') = \int_0^L dz' G(z,t,z',t') C(z') e^{iqz'} = \int_{-\infty}^{\infty} dt'' \int_0^L dz' G(z,t,z',t'') C(z') e^{iqz'} \delta(t' - t'').$$

$G'(z,t,t_0)$ can be understood as a solution for

$$\frac{\partial^2 G'(z,t,t_0)}{\partial t^2} + \Gamma \frac{\partial G'(z,t,t_0)}{\partial t} - v^2 \frac{\partial^2 G'(z,t,t_0)}{\partial z^2} = C(z) e^{iqz} \delta(t - t_0), \tag{3}$$

in which the external force, spatially distributed as $C(z)e^{iqz}$, is impulsively induced in the 1D medium at the time $t = t_0$. We can obtain $U_\Omega(z,t)$ by using a solution for Eq. (3).

B. Brillouin gain

Here we derive a Brillouin gain spectrum involved in the solution of $U_\Omega(z,t)$. This treatment is based on the stimulated amplification process of classical nonlinear optics [21,22]. In our model, the pump beam approaches the probe beam from the opposite side. The electric fields for the probe and pump beams can be treated as plane harmonic waves, which can be written as

$$\tilde{E}_1(z,t) = A_1(z,t) e^{ik_1 z - i\omega_1 t} + \text{c.c.} \tag{4}$$

and

$$\tilde{E}_2(z,t) = A_2(z,t) e^{-ik_2 z - i\omega_2 t} + \text{c.c.}, \tag{5}$$

respectively. A_i ($i = 1, 2$) is the complex amplitude of the field. We consider the wave equation for the probe beam in the medium as

$$\frac{\partial^2 \tilde{E}_1}{\partial z^2} - \frac{n^2}{c^2} \frac{\partial^2 \tilde{E}_1}{\partial t^2} = \frac{4\pi}{c^2} \frac{\partial^2 \tilde{P}_1}{\partial t^2}. \tag{6}$$

In Eq. (6), the rhs is the driving term from the nonlinear polarization $\tilde{P}_1$. $\tilde{P}_1$ couples with the sound wave U in the relationship

$$\tilde{P}_1 = \gamma U_\Omega \tilde{E}_2 = p_1 e^{-i\omega_1 t} + \text{c.c.}, \tag{7}$$

where $p_1 = \gamma u A_2 e^{-ik_2 z - i\omega_2 t} e^{i\omega_1 t} = \gamma u A_2 e^{-ik_2 z + i\Omega t}$, $U = u + \text{c.c.}$ for real U, and γ is a proportionality constant (e.g., the electrostrictive constant), since in the process of stimulated Brillouin scattering, sound waves are generated by the pump and probe beams, U, and u are given by the second order of the electric fields relating to each beam. Hence, taking into account Eq. (7), $\tilde{P}$ is a third-order quantity of the electric field. We can obtain a linearized equation for A_1 by substituting $\tilde{P}_1$ and Eq. (4) into Eq. (6) and assuming the slowly varying

approximation ($\partial^2/\partial z^2 = 0, \partial^2/\partial t^2 = 0$) to obtain

$$\left[2ik_1\frac{\partial A_1}{\partial z} - k_1^2 A_1 + \frac{n^2}{c^2}\left\{2i\omega_1\frac{\partial A_1}{\partial t} + \omega_1^2 A_1\right\}\right]e^{ik_1 z} = -\frac{4\pi}{c^2}\left[2i\omega_1\frac{\partial p_1}{\partial t} + \omega_1^2 p_1\right], \quad (8)$$

where we only consider the terms oscillating with $e^{-i\omega_1 t}$. If we also consider that the stimulated Brillouin process is in a steady state and thus $\partial/\partial t = 0$, then this formula can be simplified as follows:

$$\frac{dA_1}{dz} = i\frac{2\pi\omega_1}{cn}p_1 e^{-ik_1 z} = i\frac{2\pi\omega_1}{cn}\gamma u A_2 e^{-iqz+i\Omega t}, \quad (9)$$

where $\frac{c}{n} = \frac{\omega_1}{k_1}$. One can obtain the spatial change of the probe beam intensity $I_1 = 2nc\varepsilon_0 A_1 A_1^*$ by rewriting this differential equation as follows:

$$\frac{dI_1}{dz} = -8\pi\varepsilon_0\omega_1\gamma\,\mathrm{Im}[uA_1^* A_2 e^{-iqz+i\Omega t}]. \quad (10)$$

The average intensity of the gain probe beam in the medium is thus given by integrating Eq. (10) along a sample length L and measurement time T as follows:

$$\bar{I}_1 = I_1(0) - 8\pi\varepsilon_0\omega_1\gamma\frac{1}{T}\mathrm{Im}\int_0^L dz\int_0^T dt\,uA_1^* A_2 e^{-iqz}e^{i\Omega t}. \quad (11)$$

Note that the probe beam experiences a gain in the medium when there is sound wave u oscillating spatially and temporally with q and Ω, respectively.

C. Impulsively induced phonon

Here we consider Eq. (3) with the impulsive external force. The impulsive force is induced in the system at $t = t_0$ and provides the initial condition. Now, we integrate both sides of Eq. (3) from $t = t_0 - 0$ to $t = t_0 + 0$ to identify an effect of the impulsive force on the initial condition, and thus, we have

$$\frac{\partial G'(z,t,t_0)}{\partial t}\Big|_{t=t_0-0}^{t=t_0+0} + \Gamma G'(z,t,t_0)\Big|_{t=t_0-0}^{t=t_0+0} = C(z)e^{iqz}. \quad (12)$$

By assuming that $G'(z,t,t_0) = 0$ and $\partial G'(z,t,t_0)/\partial t = 0$ when $t < t_0$, we can obtain

$$\frac{\partial G'(z,t_0+0,t_0)}{\partial t} + \Gamma G'(z,t_0+0,t_0) = C(z)e^{iqz}. \quad (13)$$

Next, we consider that the sound wave propagates in the medium with exponential damping in the temporal domain. We can separate the exponential decay term of $G'(z,t,t_0)$ such that

$$G'(z,t,t_0) = f(qz \pm qvt)\exp\left(-\frac{\Gamma}{2}t\right), \quad (14)$$

where $f(qz \pm qvt)$ represents a forward- $(-)$ or backward $(+)$ propagating wave and Γ is the damping parameter introduced phenomenologically. By substituting G' into Eq. (13), we obtain

$$\pm qvf'(qz) + \frac{\Gamma}{2}f(qz) = C(z)e^{iqz},$$

and thus, assuming that the frequency of the sound wave is much higher than the damping, i.e., $qv = \omega \gg \Gamma$, we have

$$\pm qvf'(qz) = C(z)e^{iqz},$$

where $f'(x)$ is a derivative function of $f(x)$. One can then formally integrate for f,

$$\begin{aligned} f(qz) &= \pm\frac{1}{qv}\int C(z)e^{iqz}d(qz) + C(0) \\ &\simeq \pm\frac{1}{qv}C(z)\int e^{iqz}d(qz) + C(0) \\ &= \mp\frac{i}{qv}C(z)e^{iqz} + C(0). \end{aligned}$$

In the second line, an approximate $C(z)$ is removed from the integral because $C(z)$, which is the distribution of the laser intensities along the path of the sound wave, changes slowly compared to the wave number q. Since $C(0)$ of the second term is not oscillating, this term does not affect Eq. (11). Thus, we consider the contribution from only the first term hereafter. Therefore, we can expand the form $G'(z,t,t_0)$ as

$$G'(z,t,t_0) = \mp\frac{i}{qv}C(z \pm v(t-t_0))e^{iq[z\pm v(t-t_0)]}e^{[-\frac{\Gamma}{2}(t-t_0)]}. \quad (15)$$

This form $G'(z,t,t_0)$ denotes that the sound waves that have an envelope of $C(z)$ are generated at $t = t_0$ and propagate toward the plus and minus directions on the z axis.

D. Sound-wave reflection

Here we consider a situation in which the sound wave reflects at the crystalline surfaces and is confined in a 1D medium. The 1D medium has surfaces at $z = 0$ and $z = L$, which serve as free ends for the sound wave. In general, a wave reflected at a free end changes its propagation direction but not its phase. After twice reflecting and traveling a distance of $2L$, the wave will return to the same position and propagate in the initial direction, but a decrease in the amplitude is observed due to the attenuation. Now, we modify the formulation of the wave obtained in Eq. (15) to consider the reflection. The number of complete reflections can be written as follows:

$$n = \mathrm{floor}\left(\frac{z - vt}{L}\right), \quad (16)$$

where $\mathrm{floor}(x)$ returns the largest integer not greater than x. The formulation of the reflected waves depends on whether n is even or odd; in the even case, where $n = 2m$ (where m is a natural number),

$$G'_n(z,t,t_0) = \mp\frac{i}{qv}C(z \pm v(t-t_0) + 2Lm) \times e^{iq[z\pm v(t-t_0)+2Lm]}e^{[-\frac{\Gamma}{2}(t-t_0)]},$$

and in the odd case, where $n = 2m + 1$,

$$G'_n(z,t,t_0) = \mp\frac{i}{qv}C(-z \pm v(t-t_0) + 2L(m+1)) \times e^{iq[-z\pm v(t-t_0)+2L(m+1)]}e^{[-\frac{\Gamma}{2}(t-t_0)]}.$$

Therefore, there are four types of waves among which the phases and propagation directions are different, i.e., $qz+\Omega t$, $qz-\Omega t$, $-qz+\Omega t$, and $-qz-\Omega t$. Those may exist in a crystal after the wave is generated by the impulsive force. According to Eq. (11), we found that only the wave written as $qz-\Omega t$ can contribute to the Brillouin gain. Therefore, the effective G'_n for Brillouin gain is represented as follows:

$$G'_n(z,t,t_0) = \frac{i}{qv} C(z - v(t-t_0) + 2Lm) \times e^{iq[z-v(t-t_0)+2Lm]} e^{-\frac{\Gamma}{2}(t-t_0)} \quad \text{for } n = 2m. \quad (17)$$

The total effective wave train that will exist in the 1D medium is given by the summation over m. That is,

$$G'(z,t,t_0) = \sum_m G'_{2m}(z,t,t_0) = \frac{i}{qv} e^{iq[z-v(t-t_0)]} e^{[-\frac{\Gamma}{2}(t-t_0)]} \times \sum_m C(z - v(t-t_0) + 2Lm) e^{2iqLm}, \quad (18)$$

where

$$C(z) = \begin{cases} 0, & z < 0 \quad \text{or} \quad z > L \\ C(z), & 0 < z < L. \end{cases} \quad (19)$$

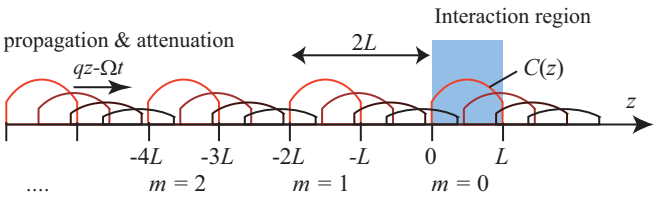

FIG. 2. (Color online) Mirror image of $G'(z,t,t_0)$ due to reflection. The $C(z)$-shaped waves propagate along the z axis with decreasing amplitude and a separation between each wave of $2L$.

This form denotes that the reflected images of the wave are periodically located on the z axis with a separation of $2L$, and they propagate in the z direction with decreasing amplitude. This behavior is shown schematically in Fig. 2.

E. Brillouin signal formulation

We discuss here the formation of the Brillouin gain signal given by Eq. (11) in the situation where the wave propagates repeatedly upon reflection within the medium. We start from the integral of the second term of the rhs in Eq. (11) to obtain the Brillouin signal. With respect to Eq. (3), the integral can be written as follows:

$$\begin{aligned} \frac{1}{T}\int_0^L\int_0^T uA_1^*A_2 e^{-iqz}e^{i\Omega t}dtdz &= \frac{i}{qvT}\int_0^L dz\int_0^T dt\int_{-\infty}^{\infty} dt' e^{i(\Omega-qv)(t-t')}e^{[-\frac{\Gamma}{2}(t-t')]}\sum_m C(z-v(t-t')+2Lm)e^{2iqLm}A_1^*A_2 \\ &= \frac{i}{qvT}\int_0^L dzT\int_{-\infty}^{\infty} ds e^{i(\Omega-qv)s}e^{(-\frac{\Gamma}{2}s)}\sum_m C(z-vs+2Lm)e^{2iqLm}A_1^*A_2 \\ &= \frac{i}{qv}\sum_m\int_{-\infty}^{\infty} ds e^{i(\Omega-qv)s}e^{-\frac{\Gamma}{2}s}e^{2iqLm}\int_0^L dzC(z-vs+2Lm)A_1^*A_2. \end{aligned} \quad (20)$$

In the above calculation, we transformed the integration variable such that

$$\int_0^T dt\int_{-\infty}^{\infty} dt' f(t-t') \Longrightarrow T\int_{-\infty}^{\infty} ds f(s). \quad (21)$$

The integral $\int_0^L dzC(z-vs+2Lm)A_1^*A_2$ in Eq. (20) depends on the range of s as follows:

$$\int_0^L dzC(z-vs+2Lm)A_1^*A_2 = \begin{cases} 0, & s < (2m-1)\frac{L}{v} \\ \int_0^{vs-2Lm+L} dzC(z-vs+2Lm)A_1^*A_2, & (2m-1)\frac{L}{v} < s < 2m\frac{L}{v} \\ \int_{vs-2Lm}^L dzC(z-vs+2Lm)A_1^*A_2, & 2m\frac{L}{v} < s < (2m+1)\frac{L}{v} \\ 0, & (2m+1)\frac{L}{v} < s. \end{cases}$$

Using this relation, Eq. (20) can be written as follows:

$$\begin{aligned} (20) = \frac{i}{qv}\sum_{m=0}\Bigg[&\int_{(2m+1)\frac{L}{v}}^{(2m+2)\frac{L}{v}} ds e^{[i(\Omega-qv)-\frac{\Gamma}{2}]s}e^{2iqL(m+1)}\int_0^{vs-2Lm-L} dzC(z-vs+2L(m+1))A_1^*A_2 \\ &+\int_{2m\frac{L}{v}}^{(2m+1)\frac{L}{v}} ds e^{[i(\Omega-qv)-\frac{\Gamma}{2}]s}e^{2iqLm}\int_{vs-2Lm}^L dzC(z-vs+2Lm)A_1^*A_2\Bigg]. \end{aligned}$$

We now elaborate on the details of $C(z)$. $C(z)$ originates in the envelope of the external force induced by the interference between the electric fields of the lasers E_1 and E_2 counterpropagating in the medium. Hence, $C(z)$ or its complex conjugate $C^*(z)$ can be written in proportion to the amplitude of each electric fields as follows:

$$A_1^*(z)A_2(z) = \beta C^*(z), \quad (22)$$

where β is a complex constant in general. The argument of β depends on the elementary process of coupling between the light and sound waves. For example, the argument for the case of coupling by electrostriction differs from that for coupling by thermal striction by 90° [14,22]. Hereafter, we treat β as a real number by assuming only an electrostriction process. Consequently, Eq. (20) can be written with β and $C(z)$ and rewritten as follows:

$$\begin{aligned}(20) = \frac{i\beta}{qv}\sum_{m=0}\Bigg[&\int_{(2m+1)\frac{L}{v}}^{(2m+2)\frac{L}{v}} ds e^{[i(\Omega-qv)-\frac{\Gamma}{2}]s} e^{2iqL(m+1)} \int_0^{vs-2Lm-L} dz C(z-vs+2L(m+1))C^*(z)\\ &+\int_{2m\frac{L}{v}}^{(2m+1)\frac{L}{v}} ds e^{[i(\Omega-qv)-\frac{\Gamma}{2}]s} e^{2iqLm} \int_{vs-2Lm}^{L} dz C(z-vs+2Lm)C^*(z)\Bigg]\\ = \frac{i\beta}{qv}&\left[\frac{1}{1-e^{(2i\Omega\tau-\Gamma\tau)}}\right]\Bigg[e^{(i\Omega-\frac{\Gamma}{2})2\tau}\int_0^{\tau} ds' e^{-[i(\Omega-qv)-\frac{\Gamma}{2}]s'}\int_{vs'}^{L} dz C(z)C^*(z-vs')\\ &+\int_0^{\tau} ds' e^{[i(\Omega-qv)-\frac{\Gamma}{2}]s'}\int_{vs'}^{L} dz C(z-vs')C^*(z)\Bigg].\end{aligned}$$

In this deformation, we used the relationship $L/v = \tau$ and transformed the integrals using the substitution of $s - 2m\tau = s'$ and the summation over m. In our case, since the laser beams are in the TEM_{00} mode and focused smoothly in the medium, $C(z)$ may be assumed to be a real function, while if either of the laser beams is transverse multimodal, $C(z)$ has to be treated as a complex function. For a real $C(z)$, the form becomes simpler:

$$(20) = \frac{i\beta}{qv}\left[\frac{1}{1-e^{(2i\Omega\tau-\Gamma\tau)}}\right]\left[\int_0^{\tau} ds'\left\{e^{(i\Omega-\frac{\Gamma}{2})2\tau}e^{-[i(\Omega-qv)-\frac{\Gamma}{2}]s'}+e^{[i(\Omega-qv)-\frac{\Gamma}{2}]s'}\right\}\int_{vs'}^{L} dz C(z)C(z-vs')\right].$$

Therefore, we can write the intensity change of the probe beam in the medium, i.e., Eq. (11), as follows:

$$\bar{I}_1 - I_1(0) \propto -\mathrm{Im}\frac{i\beta}{1-e^{2i\Omega\tau-\Gamma\tau}}\int_0^{\tau} ds'\left[\left\{e^{(i\Omega-\frac{\Gamma}{2})2\tau}e^{-[i(\Omega-qv)-\frac{\Gamma}{2}]s'}+e^{[i(\Omega-qv)-\frac{\Gamma}{2}]s'}\right\}\int_{vs'}^{L} dz C(z)C(z-vs')\right]. \tag{23}$$

This expression is the main result of this paper. Note that one can easily find the real-part formula of a Brillouin spectrum as obtained by a FM technique [9] by taking the real part of the rhs of Eq. (23) instead of the imaginary part.

Next, we try to obtain the spectral shape of the Brillouin gain spectra in various propagation cases.

F. Short-range propagation

When the propagation distance of a sound wave is much shorter than the sample length L of a medium or much shorter than the typical length of the interaction area for $C(z)$, one can assume that $\Gamma\tau \gg 1$. In this situation, the first term in $\{\cdot\}$ of the integral for s' in Eq. (23) becomes negligible compared to the second term. Consequently, since the contribution of the second term to the integral is dominant at $s' \sim 0$ and decreases with increasing s', we can use the following approximation:

$$\int_{vs'}^{L} dz C(z)C(z-vs') \sim \int_0^{L} dz C(z)C(z) = \text{const}$$

in the integral. Hence, we can obtain a simple form of the Brillouin gain spectrum as follows:

$$\bar{I}_1 - I_1(0) \propto -\mathrm{Re}\,\beta\int_0^{\tau} ds' e^{[i(\Omega-qv)-\frac{\Gamma}{2}]s'} \sim \mathrm{Re}\,\frac{\beta}{i(\Omega-qv)-\frac{\Gamma}{2}} = \frac{-\beta\left(\frac{\Gamma}{2}\right)}{(\Omega-qv)^2+\left(\frac{\Gamma}{2}\right)^2}.$$

This form reproduces a traditional Lorentzian spectrum for Brillouin scattering [22]. Note that if the β is a complex constant, the imaginary part of β yields a dispersive spectrum.

G. Coaxial propagation

Here we treat the sound wave propagating for the longer distance than the sample thickness. In Fig. 4, we summarize a variety of the considered situations. The left column of the figure shows the schematic configuration of the incident laser beams and the generated sound wave. In the right column, the intensity distributions of the electric field experienced by the propagating sound wave are depicted for each case.

Initially, we consider the simplest situation in which the beam width and power density of the laser beams are uniform within the medium, and the sound wave propagates coaxially with the laser beam, as shown in Fig. 4(a). This condition is satisfied by propagation in isotropic media or along a highly symmetric direction, even in anisotropic media. In such a situation, we begin

by assuming that $C(z) = C$, where C is a constant value such that

$$\int_{vs'}^{L} dz C(z)C(z - vs') = C^2(L - vs') = LC^2\left(1 - \frac{s'}{\tau}\right). \tag{24}$$

Then, the Brillouin gain spectra can be written as follows:

$$\begin{aligned}\bar{I}_1 - I_1(0) &\propto \mathrm{Im}\left[\frac{i\beta}{1 - e^{(2i\Omega\tau - \Gamma\tau)}}\right]\left[LC^2\int_0^{\tau} ds'\left\{e^{(i\Omega - \frac{\Gamma}{2})2\tau}e^{-[i(\Omega - qv) - \frac{\Gamma}{2}]s'} + e^{[i(\Omega - qv) - \frac{\Gamma}{2}]s'}\right\}\left(1 - \frac{s'}{\tau}\right)\right] \\ &= \mathrm{Re}\ \beta v C^2 \frac{-e^{-i(qv - \Theta)\tau} - e^{i(qv + \Theta)\tau} + e^{2i\Theta\tau}[1 + i(qv - \Theta)\tau] + 1 - i(qv - \Theta)\tau}{(1 - e^{2i\Theta\tau})(qv - \Theta)^2},\end{aligned} \tag{25}$$

where $\Theta = \Omega + i\frac{\Gamma}{2}$.

In Fig. 3, we show the spectral shape of this function which depends on the acoustic attenuation. Here, we use the parameters $qv = 20$ and $\tau = L/v = 100$ for the numerical calculation. The acoustic attenuation $\Gamma/2$, which corresponds to the original Brillouin width in a medium, was given by 0.001, 0.01, and 0.1, and the results are shown by the red, green, and blue curves, respectively. When $\Gamma\tau > 1$ (blue curve), the shape is very similar to the Lorentz function. The function is modulated with decreasing $\Gamma\tau$, as shown by the green curve. Finally, the spectrum becomes multipeaked when $\Gamma\tau < 1$ (red curve). The center region of the spectrum is enlarged in the inset and presented together with a simple Lorentz function having the same attenuation. We found that the one peak in the multipeak structure has the same linewidth as a simple Lorentzian (given as a gray curve). The origin of the multipeak structure is based on the term $1 - e^{2i\Theta\tau}(=1 - e^{2i(\Omega + i\frac{\Gamma}{2})\tau})$ in the denominator of the rhs of Eq. (25). When the condition $2\tau\Omega = 2\pi n$ is satisfied, the term takes a minimal value, which results in the peak in the spectral shape. Consequently, the peak interval $\Delta\omega$ can be obtained as follows:

$$\Delta\omega = \frac{2\pi}{2\tau} = 2\pi\frac{v}{2L}. \tag{26}$$

Note that this relation is identical to the free spectral range of a Fabry-Pérot interferometer with the velocity of sound

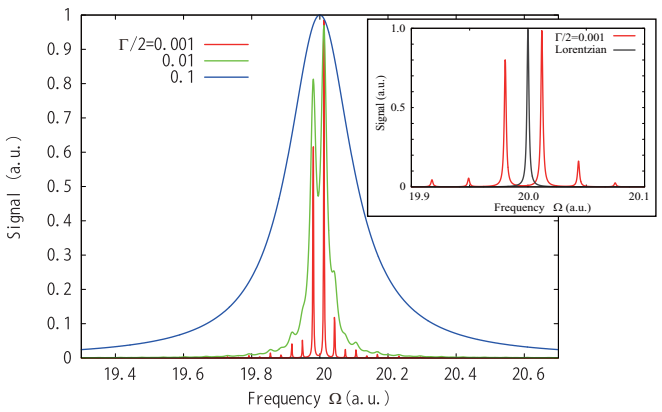

FIG. 3. (Color online) Spectral shapes of the response function depending on the acoustic attenuation from Eq. (25). $\Gamma/2 = 0.001$, 0.01, and 0.1 are shown by the red, green, and blue curves, respectively. The center frequency region for the case $\Gamma/2 = 0.001$ (red curve) and the Lorentzian (gray curve) with the same attenuation is magnified in the inset.

v replacing the speed of light c. It means that the multiple reflections of the sound wave in a medium result in a multipeaked spectral structure. By comparing this interval with the envelope spectral width of $2\pi\frac{v}{L}$, which is derived from a squared sinc component in Eq. (25) as it will be shown in Eq. (30), we can obtain the Brillouin spectrum with a triplet or quadruplet structure as was previously pointed out by Sandercock [16].

H. Off-axis propagation and Gaussian distribution of laser intensity

Here we consider the case in which the electric field intensity is not uniform along the propagation of the sound wave, i.e., $C(z)$ is not constant. Some examples of nonuniform $C(z)$ are shown in Figs. 4(b)–4(d).

In Figs. 4(b) and 4(c), we consider the off-axis propagation of the sound wave in a medium. In an anisotropic medium, the propagation direction of the sound energy, corresponding to the group velocity, does not always orient to the same direction as the wave vector $\boldsymbol{q}$. In such a case, the sound wave can walk off and deviate from the laser beam. Then, at the end of the medium, the retroreflection of the sound wave can occur. In the case of Fig. 4(b), $\boldsymbol{q}$ is normal to the surface, whereas in the case of Fig. 4(c), the propagation direction is normal to the surface. In each case, the sound wave propagates across the laser beam during the multireflection. The cross section of the laser beam intensity can be described by a Gaussian.

Even for coaxial propagation, it is possible that $C(z)$ is a nonuniform function. As shown in Fig. 4(d), when the laser is focused in a medium, the power density of the laser beam depends on the position at which it is measured along the z axis. The sound wave experiences the full spatial distribution of the power density during its propagation. According to the Gaussian beam theory [23], the distribution can be approximated by a Gaussian loosely centered around a focusing point.

Nevertheless, we can conclude that a Gaussian function is suitable for approximating a realistic situation for $C(z)$ as

$$C(z) = \begin{cases} 0, & z < 0 \quad \text{or} \quad z > L \\ \exp[-a(z - z_0)^2], & 0 < z < L, \end{cases} \tag{27}$$

where a is a parameter that denotes the spatial width of the Gaussian. When $a = 0$, $C(z)$ becomes constant, as shown in the previous section. z_0 is the center position of the focusing in the medium and, in our investigation, it is assumed to be $z_0 = L/2$.

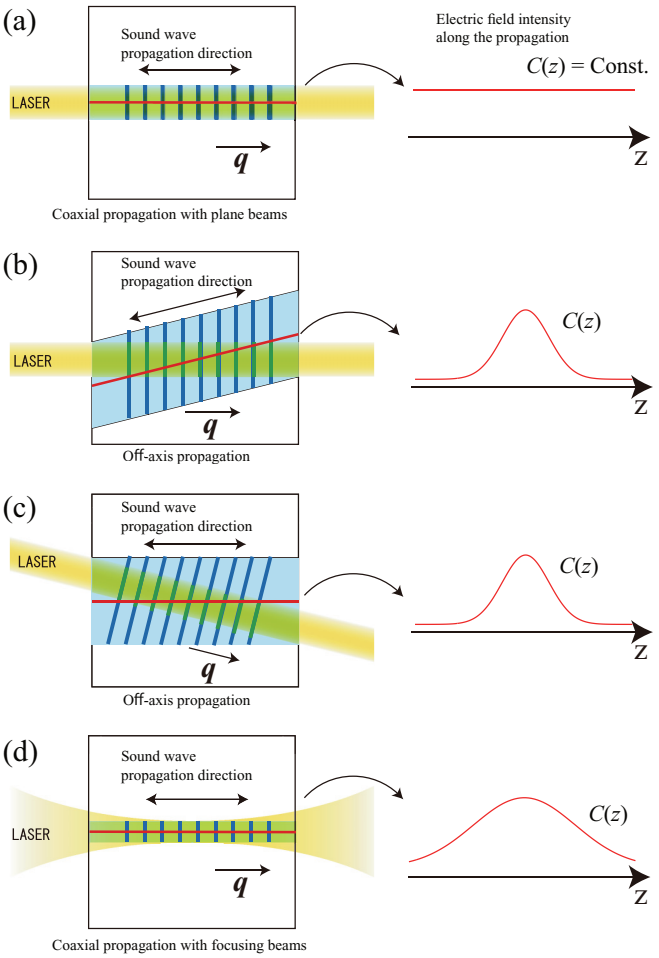

FIG. 4. (Color online) Left column: Schematic configurations of the incident laser beams and the propagating sound wave. Right column: The electric field intensity distributions experienced by the propagating sound wave. The sound wave generated by (a) plane collimated and (d) focusing beams propagates coaxially. Two types of off-axis propagation are shown in (b) and (c). (b) The sound wave walks off and deviates from the generating area in a low symmetric direction of an anisotropic media. The retroreflection of the sound wave occurs at the end of the media. (c) Even when the laser beams are misaligned from normal incidence if the crystal surface is oriented in the highly symmetric direction, the generated sound wave can propagate and multireflect.

I. Modification for parameter fitting

In this section, we attempt to modify the gain function phenomenologically to reflect the practical conditions of our experiments.

Considering that the main origin of the instrumental function is the frequency jitter of laser systems, we substituted a form of instrumental function with a Gaussian and obtained the following expression:

$$\bar{I}_1 - I_1(0) \propto \mathrm{Im}\, i\beta \int_{-\infty}^{\infty} ds e^{[i(\Omega - qv) - \frac{\Gamma}{2}]s} e^{-bs^2} \sum_m e^{2iqLm} \times \int_0^L dz C(z - vs + 2Lm) C^*(z), \quad (28)$$

where e^{-bs^2} in the integral for ds denotes the instrumental function in the time domain. In fact, the instrumental function of our measurement system is in good agreement with a Gaussian, as shown in Fig. 4 in Ref. [8].

J. Long propagation and single-time interaction

When the sound wave does not return back to its initial position after double reflection at the sample surface, the laser beams and phonon interact with each other just once, and the effective interaction length is limited by the sample length. For example, here we expect cases such that the parallelism of both of the ends of a medium is not perfect, or where the incident angle of the lasers to the surface of a sample is not precisely normal due to the misalignment of the laser beams. Our formulation for the Brillouin spectrum can be easily modified to treat such a situation.

In a consideration of a single interaction, we set $m = 0$ in Eq. (18) and rewrite the formulation as follows:

$$G'(z,t,t_0) = G'_0(z,t,t_0) = \frac{i}{qv} C(z - v(t - t_0)) e^{iq[z - v(t-t_0)]} e^{[-\frac{\Gamma}{2}(t-t_0)]}.$$

Then, Eq. (20) can be set up as follows:

$$\frac{1}{T}\int_0^L \int_0^T u A_1^* A_2 e^{-iqz} e^{i\Omega t} dt dz = \frac{i\beta}{qv} \int_0^{\frac{L}{v}} ds e^{i(\Omega - qv)s} e^{-\frac{\Gamma}{2}s} \int_{vs}^L dz C(z - vs) C^*(z). \quad (29)$$

To obtain this form, we used an integral transformation similar to the calculation in the multireflection case. This form provides us with a general form of the spectrum for a single interaction.

If $C(z) = \mathrm{const}$, it can be written in the algebraically simple form as

$$\frac{i\beta}{qv} \int_0^{\frac{L}{v}} ds e^{i(\Omega - qv)s} e^{-\frac{\Gamma}{2}s} \int_{vs}^L dz C(z - vs) C^*(z) = \frac{i\beta}{q} |C|^2 \frac{1 - e^{-i(qv - \Theta)\tau} - i(qv - \Theta)\tau}{(qv - \Theta)^2},$$

where $\tau = L/v$ and $\Theta = \Omega + i\frac{\Gamma}{2}$. When the attenuation rate is sufficiently small and we assume β is a real number, the spectrum can be written in an even simpler form as follows:

$$\bar{I}_1 - I_1(0) \propto \mathrm{Im}\, i \frac{1 - e^{-i(qv - \Omega)\tau} - i(qv - \Omega)\tau}{(qv - \Omega)^2} = \frac{\tau^2}{2} \mathrm{sinc}^2\left[\frac{(qv - \Omega)\tau}{2}\right]. \quad (30)$$

Hence, the spectral shape becomes a squared sinc function. Because the linewidth $2\pi/\tau$ is independent of Γ when $\Gamma < 1/\tau$, it is difficult to estimate the attenuation rate of the sound wave from the spectral information. It means that preparing a highly parallel sample yielding multiple reflections of the sound wave is necessary to measure the attenuation rate of the sound wave propagating a long distance in a medium of finite length. Note that this spectral shape is identified with

the spontaneous Brillouin spectra in a thin film suggested by Sandercock [16].

III. APPLICATIONS

In this section, we utilize our formulation of the Brillouin spectrum for a long-propagating wave in several experimental situations.

A. Coaxial propagation

To study the coaxial propagation, we selected the longitudinal (L) mode phonon in a TeO_2 crystal because the motivation of this investigation came from the anomalous spectral shape of this material, as reported previously [8]. TeO_2 is one of the materials commonly applied to photoelastic devices, and the elastic coefficient of the crystal is well established [24,25]. Through the elastic coefficients, we can easily calculate the pure propagation directions of the sound wave, in which the propagation direction of the energy and the wave vector are oriented in the same direction. Since the shape of the slowness surface of the (quasi) L mode in the xy plane looks like a square whose sides are tilted by 45 degrees from the xy axis, we can find that the [110] direction is one of the pure propagation directions; e.g., see Fig. 3(b) in Ref. [24]. Even if the laser beams are slightly misaligned from the normal direction to the [110] surface, the generated sound wave is expected to propagate in the [110] direction, as shown in Fig. 4(c).

We prepared a single crystal of TeO_2 whose length is 5 mm and the polished surfaces are oriented in the [110] direction. This condition is similar to the previous study [8], except the sample has a half length. We measured the temperature dependence of the Brillouin gain spectrum. The spectral shape changed with the decrease in temperature, as shown in Fig. 5. The red dots are the experimental data. The behavior of the multipeak structure at low temperatures is very similar to the previous one, except for a wide peak interval of 430 kHz. This is twice the interval frequency of the previous study, which is consistent with the thickness of the current crystal as half that of the previous TeO_2 crystal.

We applied Eq. (25) to analyze these spectra via parameter fitting. The best fit results are shown by the blue curves in the figures. The spectral change from a single peak to a multipeaked structure with decreasing temperature is clearly reproduced. From this analysis, we obtain the temperature dependence of the hypersonic attenuation in TeO_2, and the behavior of $\Gamma \propto T^{\alpha}$ ($\alpha \simeq 4$) at low temperature is consistent with the phonon-phonon scattering process of $L + L \rightarrow L$. Since further discussion is beyond the scope of this study, we will report the details in a future paper.

B. Off-axis propagation

On a demonstration of the spectral modulation caused by the off-axis propagation of the sound wave, we employed a $PbMoO_4$ crystal having the end faces of the [100] direction. $PbMoO_4$ is classified in the $4/m$ class in which the stiffness component c_{16} is nonzero. In crystals having finite c_{16}, the slowness surfaces for the modes oscillating in the xy plane are rotated around the [001] axis compared with the case of $c_{16} = 0$ [25,26]. In this case, the off-axis propagation depicted

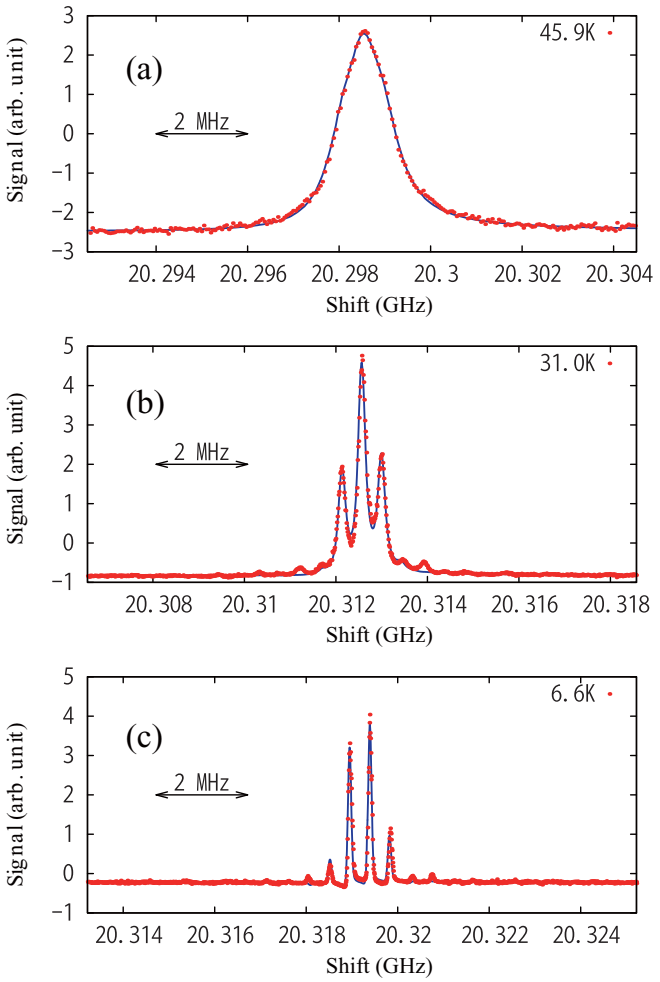

FIG. 5. (Color online) Brillouin gain spectra of TeO_2 in the [110] direction. Red points show the experimentally measured spectra at (a) 45.9, (b) 31.0, and (c) 6.6 K. The blue curves are the results of parameter fitting via Eq. (25).

in Fig. 4(b) is brought by the obliquely propagating sound wave together with wave vector $\boldsymbol{q}$ in the [100] direction; here the group velocity $\boldsymbol{v}_g$ is not parallel to $\boldsymbol{q}$.

We prepared a $PbMoO_4$ crystal with a thickness of 12 mm and measured its Brillouin gain spectra at low temperatures. A significant result is shown in Fig. 6 in which the red and blue curves are, respectively, the experimentally obtained spectra and the fitted curve based on Eqs. (23) and (27).

The spectral width of the main peak shown in Fig. 6(a) is wider than 6.5 MHz, and it is modulated in the vertical axis so seemingly noisy. However, if we expand the center region of the spectrum, as shown in Fig. 6(b), we can observe many lines of fine structures rather than a fluctuation.

As a result of the fitting procedure, the whole spectral feature consisting of a broad peak and the involved multipeak structure is reproduced very well. The obtained peak interval of 186 kHz given by fitting is reasonable in a consideration of the sound velocity in the x direction in $PbMoO_4$. At room temperature, it is 4.0×10^3 m/s and the reciprocal of the round-trip time for the 12 mm thickness is estimated to be 167 kHz. However, the sound velocity increases by

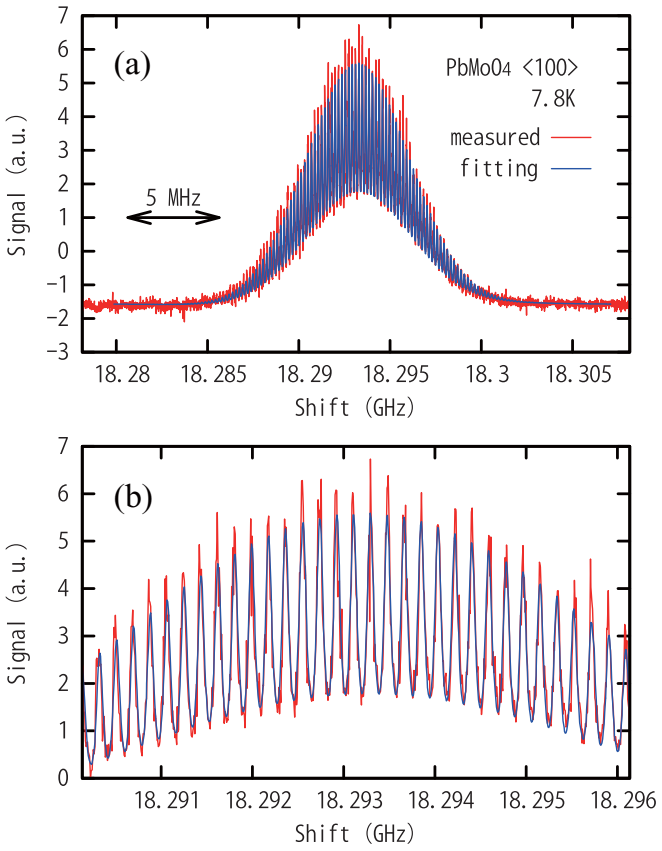

FIG. 6. (Color online) (a) Brillouin gain spectrum for $PbMoO_4$ in the [100] direction. The red curve is the experimentally obtained spectrum. The blue curve is derived from Eq. (23) by substituting Eq. (27). The center frequency region of the spectra is magnified in (b) to further clarify the fine structure present in the spectrum.

5–6% at low temperature compared to room temperature [10]. We can consider that the 6.5 MHz linewidth of the main peak corresponds to the transit time of the sound wave as it diagonally crosses the interaction region with laser beams. Note that this phenomenon in which multifine peaks are shown on a main broad peak is very similar to the phonon-resonance effect in liquids with the spontaneous Brillouin spectroscopy at the low-frequency region [17,18]. In our case, it was achieved in a crystal even at low temperatures owing to the Brillouin gain measurement concerning the phonon generated in the stimulated process.

IV. SUMMARY

We derived a formulation to describe the shape of a Brillouin gain spectrum in crystals for various temperatures. In the derivation, we assumed the 1D system where the sound wave confined in a cavity couples with laser beams of finite beam widths. This model is suitable not only for the coaxial propagation but also for the off-axis propagation of the sound wave with the laser beams. We successfully reproduced the change of Brillouin spectra in the whole temperature range obtained experimentally using TeO_2 and $PbMoO_4$ crystals under the conditions of coaxial propagation and off-axis propagation, respectively.

Our formalization of a stimulated Brillouin gain spectrum enables us to estimate the essential phonon lifetime even from the modulated spectra. It means that for investigation of the phonon physics at low temperature, it is unnecessary to prepare a sufficiently longer sample than the propagation distance. Instead, one just has to prepare a sample with high parallelism between both ends. We strongly believe that this method will further elucidate the elementary processes concerning phonon scattering in crystals.

ACKNOWLEDGMENT

This work was partially supported by JSPS KAKENHI Grant No. 26287067.

[1] W. Zhou, M. Dridi, J. Y. Suh, C. H. Kim, D. T. Co, M. R. Wasielewski, George C. Schatz, and T. W. Odom, Nat. Nanotechnol. **8**, 506 (2013).
[2] I. Ponomareva, D. Srivastava, and M. Menon, Nano Lett. **7**, 1155 (2007).
[3] A. Eichler, J. Moser, M. Dykman, and A. Bachtold, Nat. Commun. **4**, 2843 (2013).
[4] T. Czerniuk, C. Brggemann, J. Tepper, S. Brodbeck, C. Schneider, M. Kamp, S. Hfling, B. A. Glavin, D. R. Yakovlev, and A. V. A. M. Bayer, Nat. Commun. **5**, 4038 (2014).
[5] N. D. Lanzillotti-Kimura, A. Fainstein, B. Perrin, B. Jusserand, O. Mauguin, L. Largeau, and A. Lemaître, Phys. Rev. Lett. **104**, 197402 (2010).
[6] Y. Akahane, T. Asano, B.-S. Song, and S. Noda, Nature (London) **425**, 944 (2003).
[7] N. Zen, T. A. Puurtinen, T. J. Isotalo, S. Chaudhuri, and I. J. Maasilta, Nat. Commun. **5**, 3435 (2014).
[8] S. Ohno, T. Sonehara, E. Tatsu, A. Koreeda, and S. Saikan, Rev. Sci. Instrum. **77**, 123104 (2006).
[9] T. Sonehara, Y. Konno, H. Kaminaga, S. Saikan, and S. Ohno, J. Opt. Soc. Am. B **24**, 1193 (2007).
[10] T. Sonehara, E. Tatsu, S. Saikan, and S. Ohno, J. Appl. Phys. **101**, 103507 (2007).
[11] T. Sonehara, Y. Konno, H. Kaminaga, and S. Saikan, J. Korean Phys. Soc. **51**, 836 (2007).
[12] T. Sonehara, H. Kaminaga, E. Tatsu, S. Saikan, and S. Ohno, J. Non-Cryst. Solids **354**, 1768 (2008).
[13] T. Sonehara, H. Kaminaga, E. Tatsu, S. Saikan, and S. Ohno, Opt. Lett. **32**, 808 (2007).
[14] T. Sonehara, H. Kaminaga, E. Tatsu, S. Saikan, and S. Ohno, J. Appl. Phys. **101**, 073104 (2007).
[15] A. Koreeda and S. Saikan, Rev. Sci. Instrum. **82**, 126103 (2011).
[16] J. R. Sandercock, Phys. Rev. Lett. **29**, 1735 (1972).
[17] K. Sakai, K. Hattori, and K. Takagi, Phys. Rev. B **52**, 9402 (1995).
[18] Y. Minami and K. Sakai, J. Appl. Phys. **104**, 103505 (2008).
[19] P. T. Rakich, C. Reinke, R. Camacho, P. Davids, and Z. Wang, Phys. Rev. X **2**, 011008 (2012).
[20] T. Satoh, Y. Terui, R. Moriya, B. A. Ivanov, K. Ando, E. Saitoh, T. Shimura, and K. Kuroda, Nat. Photon. **6**, 662 (2012).
[21] Y. R. Shen, *The Principles of Nonlinear Optics* (Wiley-Interscience, New York, 2002).

[22] R. W. Boyd, *Nonlinear Optics* (Academic, San Diego, 1992).
[23] B. E. A. Saleh and M. C. Teich, *Fundamentals of Photonics*, 2nd ed. (Wiley-Interscience, New York, 2007).
[24] D. C. Hurley, J. P. Wolfe, and K. A. McCarthy, Phys. Rev. B **33**, 4189 (1986).
[25] D. Royer and E. Dieulesaint, *Elastic Waves in Solids I Free and Guided Propagation* (Springer-Verlag, Berlin, Heidelberg, 1999).
[26] J. Rouvaen, E. Bridoux, and R. Torguet, Appl. Phys. Lett. **22**, 619 (1973).